JOURNAL OF FUNDAMENTAL MATHEMATICS
AND APPLICATIONS (JFMA) VOL. 8 NO. 2 (2025)
Available online at www.jfma.math.fsm.undip.ac.id

STABILITY ANALYSIS OF THE MODEL $SVEI_aI_sR$ ON COVID-19 SPREAD

Tiara Adinda Permatasari[1*], Redemtus Heru Thahjana[2], Widowati[3]

[1,2,3]*Diponegoro University*
Email : [1]tiaraapermatasari@gmail.com, [2] redemtusherutjahjana@lecturer.undip.ac.id,
[3] widowati@lecturer.undip.ac.id
[*]corresponding author

Abstract. The COVID-19 pandemic has presented a major challenge in understanding the dynamics of disease transmission in a region. DKI Jakarta is the province with the highest number of COVID-19 cases in Indonesia. In this article, the $SVEI_aI_sR$ model (Susceptible, Vaccinated, Exposed, Asymptomatic, Symptomatic, and Recovered) is examined to model the spread of COVID-19 in DKI Jakarta Province. The basic reproduction number is obtained through the Next Generation Matrix (NGM) approach, whereas the local stability analysis is carried out using the Routh–Hurwitz criterion. Furthermore, there are two equilibrium points obtained, which are the disease-free equilibrium and the endemic equilibrium. The stability of the equilibrium point is analyzed based on the value of the basic reproduction number. The endemic equilibrium point is considered asymptotically stable if the basic reproduction number is less than one. To demonstrate the behavior of the COVID-19 transmission model, numerical simulations are conducted using data obtained from DKI Jakarta Province. The results of the analysis indicate that, the COVID-19 transmission model is asymptotically stable at the diseas-free equilibrium point with $\Re_0 = 0.001897843854$. This indicates that, over time, the COVID-19 disease will eventually disappear from the population.
Keywords: Basic reproduction number; Stability Analysis; Vaccination; COVID-19.

I. INTRODUCTION

SARS-CoV-2, the virus responsible for COVID-19, is a novel human-infecting strain of the coronavirus family. This virus is capable of infecting individuals of all age groups, including infants, children, adults, the elderly, as well as pregnant and lactating women. The infection caused by this virus is known as COVID-19 and was first identified in Wuhan, China, in late December 2019. SARS-CoV-2 can cause an infectious disease characterized by symptoms such as coughing, fever, loss of taste or smell, and shortness of breath. The virus can be transmitted by both symptomatic and asymptomatic infected individuals, making its spread difficult to predict [1]. Transmission by asymptomatic individuals is believed to be one of the main factors contributing to the rapid spread of the disease. COVID-19 transmission occurs through contact between an infected individual and a susceptible one, primarily via respiratory droplets expelled when an infected person coughs or sneezes.

One of the measures to control the spread of COVID-19 is through the use of mathematical modeling. Mathematical models are widely applied across various scientific fields, including health sciences, particularly in addressing infectious disease control. Mathematical modeling is a branch of mathematics that describes and explains real-world problems in mathematical form, allowing for a more precise understanding of those problems [2]. Furthermore, to describe continuous changes in population dynamics over time, mathematical modeling can be

employed—for example, in studying the spread of infectious diseases, where mathematical models play an essential role in analyzing disease transmission and control [3].

In studying the transmission of COVID-19, several common mathematical models have been widely used, including the SIS, SIR, and SEIR models. These models are employed to predict the epidemiological dynamics of COVID-19 transmission. Several previous studies have proposed various modifications of these basic models. For instance, the SVEAIR model proposed by Zhong Hua Shen et al. [4] incorporates control measures such as self-isolation, vaccination, and rapid testing. Another study by Naba Kumar Goswami et al. [5] introduced the $\mathrm{SEQI_aI_sMR}$ model, which considers control strategies including self-protection, medical facility inspection and treatment, and administration of medication to infected individuals. The $\mathrm{SEI_1I_2QR}$ model proposed by Jiraporn Lamwong et al. [6] includes social distancing, mask usage, and vaccination as control measures. M. Aakash et al. [7] proposed the SEIDQR model, considering control variables such as treatment, quarantine, and deduction efficacy. Similarly, Ammar ElHasan et al. [8] introduced the SEIQR model, which includes self-protection as a control variable. Anip Kumar Paul et al. [9] developed the $\mathrm{SV_aV_bB_VEAIN_hHR}$ model, which divides vaccinated individuals into three groups based on the number of vaccine doses received. Meanwhile, Shraddha Ramdas Bandekar and Mini Ghosh [10] proposed the SS_qEIH_qHR model, employing self-protection measures to reduce disease transmission, along with rapid testing and contact tracing to detect both symptomatic and asymptomatic individuals. Furthermore, Nurul Aini Istiqomah et al. [11] proposed the STQIR model, which considers physical distancing and self-protection measures as part of the model parameters, while U. A. Fitriani et al. [12] proposed another STQIR model that includes self-protection, treatment, and quarantine as control variables. In addition, Omar Forrest et al. [13] proposed the SVIR model, which considers vaccination as the primary control measure. Lastly, Kaijing Chen et al. [14] introduced the SVEIR model, which distinguishes the Exposed and Infected subpopulations based on new COVID-19 variants, and Mo'tassem Al Arydah [15] proposed the SVIRD model, incorporating optimal vaccination control.

In this article, the SVEAIR model developed by Hussain *et al.* [16] is extended by introducing an interaction between asymptomatic and symptomatic infected individuals. After constructing the model, the basic reproduction number ($\Re_0$) is calculated to investigate the transmission rate of COVID-19. The analysis is then carried out to determine the stability of both the disease-free and endemic equilibrium states. To validate the effectiveness of the proposed model, numerical simulations are performed using data obtained from DKI Jakarta Province [17]. The simulation results indicate that the disease-free equilibrium point is asymptotically stable.

II. MATHEMATICAL MODEL FORMULATION

The COVID-19 transmission model presented in this study describes the interactions among six population compartments: the susceptible subpopulation that has not received vaccination (S), the vaccinated susceptible subpopulation that has received two doses (V), the exposed subpopulation (E), the asymptomatic infected subpopulation (I_a), the symptomatic infected subpopulation (I_s), and the recovered subpopulation (R). The interactions among these six subpopulations are illustrated in the compartmental diagram shown in Fig. 1, while the descriptions of the parameters used in the model are provided in Table 1,

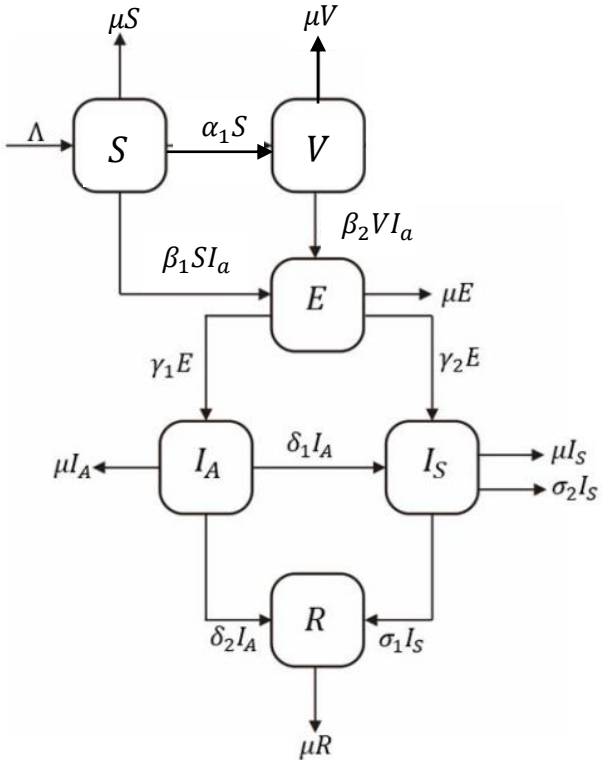

Fig. 1. Transmission Diagram of COVID-19 Disease.

Table 1. Description of Parameter in System (1)

Λ	Rate of increase of unvaccinated susceptible individuals
β_1	Interaction rate between unvaccinated susceptible and asymptomatic infected individuals
α	Vaccination rate of first and second doses for unvaccinated individuals
μ	Proportion of natural mortality in all compartments
γ_1	The proportion of exposed individuals who become asymptomatically infected
γ_2	The proportion of exposed individuals who become symptomatically infected
δ_1	The proportion of asymptomatically infected individuals who develop disease symptoms
δ_2	The recovery rate of asymptomatically infected individuals
σ_1	The recovery rate of symptomatically infected individuals
σ_2	Death rate due to infection among symptomatic individuals

The susceptible subpopulation that has not received vaccination (S) increases by Λ, representing the recruitment rate of new individuals, and decreases as a result of vaccination at a rate α, moving individuals into the vaccinated susceptible subpopulation (V). In addition, interactions between susceptible and infected individuals cause susceptible individuals to become exposed and move into the exposed subpopulation (E) at a rate β_1. The vaccinated susceptible subpopulation (V) increases as unvaccinated susceptible individuals receive vaccination at a rate α, and decreases through interactions between vaccinated susceptible and

infected individuals, causing them to become exposed and move into the exposed subpopulation at a rate β_2. The exposed subpopulation (E) increases due to interactions between unvaccinated susceptible and infected individuals at a rate β_1, and between vaccinated susceptible and infected individuals at a rate β_2. The exposed subpopulation decreases as exposed individuals progress to the asymptomatically infected subpopulation (I_a) at a rate γ_1, and to the symptomatically infected subpopulation (I_s) at a rate γ_2. In the asymptomatic infected subpopulation (I_a), the population increases due to exposed individuals becoming asymptomatic at a rate of γ_1, while it decreases as asymptomatic individuals progress to the symptomatic stage at a rate of $\delta_1$or recover at a rate δ_2. Meanwhile, the symptomatically infected subpopulation (I_s) grows when exposed individuals become symptomatic at a rate of γ_2 and when asymptomatic individuals develop symptoms at a rate δ_1. It decreases as symptomatic individuals either recover at a rate $\sigma_1$or die due to infection at a rate σ_2. The recovered subpopulation (R) increases when asymptomatic individuals recover at a rate of δ_2 and symptomatic individuals recover at a rate of σ_1. Furthermore, each subpopulation experiences natural mortality at a rate μ. In this study, the spread of COVID-19 is modeled through the following system of ordinary differential equations (1):

$$\begin{aligned}
\frac{dS}{dt} &= \Lambda - \alpha S - \beta_1 S I_a - \mu S \\
\frac{dV}{dt} &= \alpha S - \beta_2 V I_a - \mu V \\
\frac{dE}{dt} &= \beta_1 S I_a + \beta_2 V I_a - \gamma_1 E - \gamma_2 E - \mu E \\
\frac{dI_a}{dt} &= \gamma_1 E - \delta_1 I_a - \delta_2 I_a - \mu I_a \\
\frac{dI_s}{dt} &= \gamma_2 E + \delta_1 I_a - \sigma_1 I_s - \sigma_2 I_s - \mu I_s \\
\frac{dR}{dt} &= \delta_2 I_a - \sigma_1 I_s - \mu R
\end{aligned} \tag{1}$$

with initial values $S(0) > 0,\ V(0) \geq 0,\ E(0) \geq 0, I_a(0) \geq 0, I_s \geq 0, R(0) \geq 0$.

III. BASIC REPRODUCTION NUMBER

In the disease transmission model, one of the key parameters used to predict the rate of disease spread is the basic reproduction number. The basic reproduction number represents the average number of secondary infection cases generated by a single primary infection in a fully susceptible population [18]. If $\mathfrak{R}_0 > 1$, each infected person can infect more than one susceptible individual, allowing the disease to spread through the population and making the disease-free equilibrium unstable, which can result in an epidemic [1]. On the other hand, if $\mathfrak{R}_0 < 1$, each infected person infects fewer than one susceptible individual, so the disease cannot spread, and the disease-free equilibrium becomes asymptotically stable [19]. The basic reproduction number can be determined using the Next Generation Matrix method. The infected compartments in this study are denoted by $E, I_a, I_s,$ and R. Let $x = (E, I_a, I_s, R)$, so that system (1) can be rewritten as follows:

$$\frac{dx}{dt} = F(x) - V(x) \qquad ,x = [E, I_a, I_s, R]^T$$

where $F(x)$ represents the matrix containing individuals newly infected with the COVID-19 virus at the initial stage, and $V(x)$ represents the matrix containing actively infected individuals, as follows:

$$F(x) = \begin{bmatrix} F_1 \\ F_2 \\ F_3 \\ F_4 \end{bmatrix} = \begin{bmatrix} \beta_1 S I_a + \beta_2 V I_a \\ 0 \\ 0 \\ 0 \end{bmatrix}, V(x) = \begin{bmatrix} V_1 \\ V_2 \\ V_3 \\ V_4 \end{bmatrix} = \begin{bmatrix} \gamma_1 E + \gamma_2 E + \mu E \\ \delta_1 I_a + (\delta_2 + \mu) I_a - \gamma_1 E \\ (\sigma_1 + \sigma_2) I_s + \mu I_s - \gamma_2 E - \delta_1 I_a \\ \mu R + \sigma_1 I_s - \delta_2 I_a \end{bmatrix}$$

Next, the Jacobian matrices $\mathcal{F}$and $\mathcal{V}$will be determined.

$$\mathcal{F} = \begin{bmatrix} \frac{\partial F_1}{\partial E} & \frac{\partial F_1}{\partial I_a} & \frac{\partial F_1}{\partial I_s} & \frac{\partial F_1}{\partial R} \\ \frac{\partial F_2}{\partial E} & \frac{\partial F_2}{\partial I_a} & \frac{\partial F_2}{\partial I_s} & \frac{\partial F_2}{\partial R} \\ \frac{\partial F_3}{\partial E} & \frac{\partial F_3}{\partial I_a} & \frac{\partial F_3}{\partial I_s} & \frac{\partial F_3}{\partial R} \\ \frac{\partial F_4}{\partial E} & \frac{\partial F_4}{\partial I_a} & \frac{\partial F_4}{\partial I_s} & \frac{\partial F_4}{\partial R} \end{bmatrix} = \begin{bmatrix} 0 & \beta_1 S + \beta_2 V & 0 & 0 \\ 0 & 0 & 0 & 0 \\ 0 & 0 & 0 & 0 \\ 0 & 0 & 0 & 0 \end{bmatrix}$$

$$\mathcal{V} = \begin{bmatrix} \frac{\partial V_1}{\partial E} & \frac{\partial V_1}{\partial I_a} & \frac{\partial V_1}{\partial I_s} & \frac{\partial V_1}{\partial R} \\ \frac{\partial V_2}{\partial E} & \frac{\partial V_2}{\partial I_a} & \frac{\partial V_2}{\partial I_s} & \frac{\partial V_2}{\partial R} \\ \frac{\partial V_3}{\partial E} & \frac{\partial V_3}{\partial I_a} & \frac{\partial V_3}{\partial I_s} & \frac{\partial V_3}{\partial R} \\ \frac{\partial V_4}{\partial E} & \frac{\partial V_4}{\partial I_a} & \frac{\partial V_4}{\partial I_s} & \frac{\partial V_4}{\partial R} \end{bmatrix} = \begin{bmatrix} \gamma_1 + \gamma_2 + \mu & 0 & 0 & 0 \\ -\gamma_1 & \delta_1 + \delta_2 + \mu & 0 & 0 \\ -\gamma_2 & -\delta_1 & \sigma_1 + \sigma_2 + \mu & 0 \\ 0 & -\delta_2 & -\sigma_1 & \mu \end{bmatrix}$$

The Jacobian matrices $\mathcal{F}$ and $\mathcal{V}$ are obtained by evaluating the functions $F(x)$ and $V(x)$ at the disease-free equilibrium pointThen, by substituting the value of the disease-free equilibrium point $\mathcal{E}^0(S_0, V_0, E_0, I_{a_0}, I_{s_0}, R_0) = (\frac{\Lambda}{\alpha+\mu}, \frac{\Lambda\alpha}{\mu(\alpha+\mu)}, 0,0,0,0)$ into the matrix F, we obtain:

$$\mathcal{F}(\mathcal{E}_0) = \begin{bmatrix} 0 & \frac{\beta_1 \Lambda}{\alpha+\mu} + \frac{\beta_2 \Lambda \alpha}{\mu(\alpha+\mu)} & 0 & 0 \\ 0 & 0 & 0 & 0 \\ 0 & 0 & 0 & 0 \\ 0 & 0 & 0 & 0 \end{bmatrix},$$

Then, the eigenvalues of the NGM matrix are determined, where the Next Generation Matrix is given by $NGM = \mathcal{F}(\mathcal{E}_0).\mathcal{V}^{-1}$ and the result is obtained as follows:

$$NGM = \begin{bmatrix} g_{11} & g_{12} & 0 & 0 \\ 0 & 0 & 0 & 0 \\ 0 & 0 & 0 & 0 \\ 0 & 0 & 0 & 0 \end{bmatrix}$$

with

$$g_{11} = \frac{\left(\frac{\beta_1 \Lambda}{\alpha+\mu} + \frac{\beta_2 \Lambda \alpha}{\mu(\alpha+\mu)}\right)\gamma_1}{(\gamma_1 + \gamma_2 + \mu)\,(\delta_1 + \delta_2 + \mu)}, g_{12} = \frac{\frac{\beta_1 \Lambda}{\alpha+\mu} + \frac{\beta_2 \Lambda \alpha}{\mu(\alpha+\mu)}}{\delta_1 + \delta_2 + \mu}$$

The transmission rate of COVID-19 within a population shows how fast the virus spreads and helps determine the measures needed to prevent further infections, or the spectral radius of the NGM, $\mathfrak{R}_0$ is obtained as follows:

$$\mathfrak{R}_0 = \frac{\Lambda\gamma_1(\alpha\beta_2 + \mu\beta_1)}{\mu(\gamma_1 + \gamma_2 + \mu)(\delta_1 + \delta_2 + \mu)(\alpha + \mu)}.$$

IV. EQUILIBRIUM POINT

An equilibrium point refers to a stable state of the system achieved at a particular point. The COVID-19 transmission model attains equilibrium if the condition below is fulfilled:

$$\frac{dS}{dt} = 0, \frac{dV}{dt} = 0, \frac{dE}{dt} = 0, \frac{dI_a}{dt} = 0, \frac{dI_s}{dt} = 0, \frac{dR}{dt} = 0 \quad (2)$$

System (1) has two equilibrium points: the endemic equilibrium (EE), denoted by $\mathcal{E}^*(S^*, V^*, E^*, I_a{}^*, I_s{}^*, R^*)$ and the disease-free equilibrium (DFE), denoted by $\mathcal{E}^0(S_0, V_0, E_0, I_{a0}, I_{s0}, R_0) = (\frac{\Lambda}{\alpha+\mu}, \frac{\Lambda\alpha}{(\alpha+\mu)(\beta_2+\mu)}, 0,0,0,0)$. Maple software was used to assist in finding the endemic equilibrium of System (1), and the endemic equilibrium $\mathcal{E}^* = (S^*, V^*, E^*, I_a{}^*, I_s{}^*, R^*)$ was obtained as follows:

$$S^* = \frac{(\gamma_1+\gamma_2+\mu)(\delta_1+\delta_2+\mu)(\beta_2+\mu)}{\gamma_1(\alpha\beta_2+\beta_1\beta_2+\beta_1\mu)}$$

$$V^* = \frac{\alpha(\gamma_1+\gamma_2+\mu)(\delta_1+\delta_2+\mu)}{\gamma_1(\alpha\beta_2+\beta_1\beta_2+\beta_1\mu)}$$

$$E^* = \frac{1}{(\gamma_1+\gamma_2+\mu)(\beta_2+\mu)\beta_1\gamma_1}(R_0-1)$$

$$I_a^* = \frac{1}{\beta_1(\gamma_1+\gamma_2+\mu)(\delta_1+\delta_2+\mu)(\beta_2+\mu)}(R_0-1)$$

$$I_s^* = \frac{(\delta_1\gamma_1+\delta_1\gamma_2+\delta_2\gamma_2+\gamma_2\mu)}{\beta_1(\gamma_1+\gamma_2+\mu)(\delta_1+\delta_2+\mu)(\sigma_1+\sigma_2+\mu)(\beta_2+\mu)}(R_0-1)$$

$$R^* = \frac{(\delta_1\gamma_1\sigma_1+\delta_1\gamma_2\sigma_1+\delta_2\gamma_1\sigma_1+\delta_2\gamma_1\sigma_2+\delta_2\gamma_2\sigma_1+\gamma_2\mu\sigma_1)}{\beta_1\gamma_1\mu(\gamma_1+\gamma_2+\mu)(\delta_1+\delta_2+\mu)(\sigma_1+\sigma_2+\mu)(\beta_2+\mu)}(R_0-1)$$

V. STABILITY ANALYSIS

Before presenting the stability results, we first clarify the definition of stability adopted in this study. An equilibrium point is said to be locally asymptotically stable if solutions starting sufficiently close to the equilibrium converge to it as time approaches infinity, and unstable if solutions diverge from it. These definitions follow standard formulations in dynamical systems theory as presented in [20]. Based on this concept, stability analysis is carried out to determine whether a disease will spread or disappear from a population, in order to identify appropriate

further actions. The stability analysis can be performed around the disease-free equilibrium point $\mathcal{E}^0(S_0, V_0, E_0, I_{a_0}, I_{s_0}, R_0)$ and around the endemic equilibrium point $\mathcal{E}^* = (S^*, V^*, E^*, I_a{}^*, I_s{}^*, R^*)$.

The stability of the equilibrium points is then analyzed using the Jacobian matrix to calculate the eigenvalues at $\mathcal{E}^0(S_0, V_0, E_0, I_{a_0}, I_{s_0}, R_0)$. The local stability analysis of the disease-free equilibrium point of System (1) can be demonstrated based on the following theorem.

Theorem 1. Given $\mathfrak{R}_0 = \frac{\Lambda\gamma_1(\alpha\beta_2+\beta_1\beta_2+\mu\beta_1)}{(\beta_2+\mu)(\gamma_1+\gamma_2+\mu)(\delta_1+\delta_2+\mu)(\alpha+\mu)}$. If $\mathfrak{R}_0 < 1$, then the disease-free equilibrium point $\mathcal{E}^0(S_0, V_0, E_0, I_{a_0}, I_{s_0}, R_0)$ is locally asymptotically stable, whereas if $\mathfrak{R}_0 > 1$, the equilibrium point $\mathcal{E}^0(S_0, V_0, E_0, I_{a_0}, I_{s_0}, R_0)$ is unstable.

Proof :

Assume $\mathcal{E}^0(S_0, V_0, E_0, I_{a_0}, I_{s_0}, R_0) = (\frac{\Lambda}{\alpha+\mu}, \frac{\Lambda\alpha}{(\alpha+\mu)(\beta_2+\mu)}, 0,0,0,0)$. Using the following formula, the eigenvalues of the Jacobian matrix at $\mathcal{E}^0(S_0, V_0, E_0, I_{a_0}, I_{s_0}, R_0)$ are obtained:

$$|J(\mathcal{E}^0) - xI| = 0$$

After determining the eigenvalues, the characteristic equation is obtained as follows:

$$(\mu + x^2)(\mu + \sigma_1 + \sigma_2 + x)(\alpha + \mu + x)(a_0x^2 + a_1x + a_2)$$

with

$$a_0 = 1$$

$$a_1 = \delta_1 + \delta_2 + \gamma_1 + \gamma_2 + 4\mu$$

$$a_2 = \frac{1}{(\beta_2+\mu)(\alpha+\mu)}(-\gamma_1(\alpha\beta_2 + \beta_2\beta_1 + \beta_1\mu)\Lambda + (\beta_2 + \mu)(\gamma_1 + \gamma_2 + \mu)(\delta_1 + \delta_2 + \mu)(\alpha + \mu)$$

According to the Routh–Hurwitz criterion, the equilibrium point $\mathcal{E}^0(S_0, V_0, E_0, I_{a_0}, I_{s_0}, R_0)$ achieves asymptotic stability if its characteristic equation has coefficients that fulfill $a_1 > 0$ and $a_2 > 0$.

Since all model parameters are positive, the condition $a_1 > 0$ is automatically satisfied. To prove $a_2 > 0$, algebraic manipulation based on the Routh–Hurwitz criterion is carried out. This condition is fulfilled whenever $\mathfrak{R}_0 < 1$, which therefore implies that the equilibrium point is asymptotically stable.

It will be shown that $a_2 > 0$ whenever $\mathfrak{R}_0 < 1$

$$a_2 = \frac{1}{(\beta_2+\mu)(\alpha+\mu)}(-\gamma_1(\alpha\beta_2 + \beta_2\beta_1 + \beta_1\mu)\Lambda + (\beta_2 + \mu)(\gamma_1 + \gamma_2 + \mu)(\delta_1 + \delta_2 + \mu)(\alpha + \mu)$$

Since the denominator is positive, $a_2 > 0$ if the following condition is satisfied:

$$\Leftrightarrow (-\gamma_1(\alpha\beta_2 + \beta_2\beta_1 + \beta_1\mu)\Lambda + (\beta_2 + \mu)(\gamma_1 + \gamma_2 + \mu)(\delta_1 + \delta_2 + \mu)(\alpha + \mu) > 0$$

$$\Leftrightarrow \gamma_1(\alpha\beta_2 + \beta_2\beta_1 + \beta_1\mu)\Lambda < (\beta_2 + \mu)(\gamma_1 + \gamma_2 + \mu)(\delta_1 + \delta_2 + \mu)(\alpha + \mu)$$

$$\Leftrightarrow \frac{\gamma_1(\alpha\beta_2 + \beta_2\beta_1 + \beta_1\mu)\Lambda}{(\beta_2 + \mu)(\gamma_1 + \gamma_2 + \mu)(\delta_1 + \delta_2 + \mu)(\alpha + \mu)} = \mathfrak{R}_0 < 1$$

Hence, it is proven that the condition $a_2 > 0$ is satisfied if $\mathfrak{R}_0 < 1$.

The disease-free equilibrium $\mathcal{E}^0(S_0, V_0, E_0, I_{a_0}, I_{s_0}, R_0) = (\frac{\Lambda}{\alpha+\mu}, \frac{\Lambda\alpha}{(\alpha+\mu)(\beta_2+\mu)}, 0,0,0,0)$ is locally asymptotically stable if $\mathfrak{R}_0 < 1$. This indicates that each actively infected individual can transmit the disease to fewer than one susceptible person, and over time, the disease will gradually disappear from the population (disease-free state).

Theorem 2. Given $\Re_0 = \frac{\Lambda\gamma_1(\alpha\beta_2+\beta_1\beta_2+\mu\beta_1)}{(\beta_2+\mu)(\gamma_1+\gamma_2+\mu)(\delta_1+\delta_2+\mu)(\alpha+\mu)}$. If $\Re_0 > 1$, the endemic equilibrium point $\mathcal{E}^* = (S^*, V^*, E^*, {I_a}^*, {I_s}^*, R^*)$ is locally asymptotically stable, whereas if $\Re_0 > 1$, the equilibrium point $\mathcal{E}^* = (S^*, V^*, E^*, {I_a}^*, {I_s}^*, R^*)$ is unstable.

Proof :

The eigenvalues will be determined based on the Jacobian matrix at $\mathcal{E}^* = (S^*, V^*, E^*, {I_a}^*, {I_s}^*, R^*)$ using the following formula:

$$|J(\mathcal{E}^*) - xI| = 0$$

After determining the determinant of the matrix, the following characteristic equation is obtained:

$$(\mu + x)(\mu + \sigma_1 + \sigma_2 + x)(a_0x^4 + a_1x^3 + a_2x^2 + a_3x + a_4)$$

with,

$$a_0 = 1 \tag{2}$$

$$a_1 = (\beta_1 + \beta_2)I_a^* + \alpha_1 + \delta_1 + \delta_2 + \gamma_1 + \gamma_2 + 4\mu \tag{3}$$

$$\begin{aligned} a_2 = {} & \beta_1\beta_2{I_a^*}^2 + \big((\beta_1 + \beta_2)\gamma_1 + (3\mu + \gamma_2 + \alpha + \delta_1 + \delta_2)\beta_2 \\ & + (3\mu + \gamma_2 + \delta_1 + \delta_2)\beta_1\big)I_a^* \\ & + (-S^*\beta_1 - V^*\beta_2 + \alpha + \delta_1 + \delta_2 + 3\mu)\gamma_1 + 6\mu^2 \\ & + (3\gamma_2 + 3\alpha + 3\delta_1 + 3\delta_2)\mu + (\delta_2 + \gamma_2 + \delta_1)\alpha_1 + \gamma_2(\delta_1 + \delta_2) \end{aligned} \tag{4}$$

$$\begin{aligned} a_3 = {} & \big(-\beta_1\gamma_1\beta_2I_a^* - \beta_1\gamma_1(\alpha + 2\mu)\big)S^* + \big(-\beta_1\gamma_1\beta_2I_a^* - \beta_2\gamma_1(\alpha + 2\mu)\big)V^* \\ & + \beta_2(2\mu + \gamma_1 + \gamma_2 + \delta_1 + \delta_2)\beta_1{I_a^*}^2 \\ & + (\alpha\beta_2\delta_1 + \alpha\beta_2\delta_2 + \alpha\beta_2\gamma_1 + \alpha\beta_2\gamma_2 + 2\alpha\beta_2\mu + \beta_1\delta_1\gamma_1 + \beta_1\delta_1\gamma_2 \\ & + 2\beta_1\delta_1\mu + \beta_1\delta_2\gamma_1 + \beta_1\delta_2\gamma_2 + 2\beta_1\delta_2\mu + 2\beta_1\gamma_1\mu + 2\beta_1\gamma_2\mu \\ & + 3\mu^2\beta_1 + \beta_2\delta_1\gamma_1 + \beta_2\delta_1\gamma_2 + 2\beta_2\delta_1\mu + \beta_2\delta_2\gamma_1 + \beta_2\delta_2\gamma_2 + 2\beta_2\delta_2\mu \\ & + 2\beta_2\gamma_1\mu + 2\beta_2\gamma_2\mu + 3\mu^2\beta_2)I_a^* + \alpha\delta_1\gamma_1 + \alpha\delta_1\gamma_2 + 2\alpha\delta_1\mu + \alpha\delta_2\gamma_1 \\ & + \alpha\delta_2\gamma_2 + 2\alpha\delta_2\mu + 2\alpha\gamma_1\mu + 2\alpha\gamma_2\mu + 3\mu^2\alpha + 2\delta_1\gamma_1\mu + 2\delta_1\gamma_2 \\ & + 3\mu^2\delta_1 + 2\delta_2\gamma_1\mu + 2\delta_2\gamma_2\mu + 3\mu^2\delta_2 + 3\mu^2\gamma_1 + 3\mu^2\gamma_2 + 4\mu^3 \end{aligned} \tag{5}$$

$$\begin{aligned} a_4 = {} & \big(-\beta_1\gamma_1\beta_2\mu I_a^* - \beta_1\gamma_1\mu(\alpha + \mu)\big)S^* + \big(-\beta_1\gamma_1\beta_2\mu I_a^* - \beta_2\gamma_1\mu(\alpha + \mu)\big)V^* \\ & + \beta_1\beta_2(\gamma_1 + \gamma_2 + \mu)(\delta_1 + \delta_2 + \mu){I_a^*}^2 \\ & + (\gamma_1 + \gamma_2 + \mu)(\delta_1 + \delta_2 + \mu)(\alpha\beta_2 + \beta_1\mu + \beta_2\mu)I_a^* + \mu(\gamma_1 + \gamma_2 \\ & + \mu)(\delta_1 + \delta_2 + \mu)(\alpha + \mu) \end{aligned} \tag{6}$$

Based on the Routh–Hurwitz criterion, the endemic equilibrium, $\mathcal{E}^* = (S^*, V^*, E^*, {I_a}^*, {I_s}^*, R^*)$ is locally asymptotically stable when all the roots of the polynomial have negative real parts, as shown below :

$$x_1 + x_2 + x_3 + x_4 = -\frac{b}{a} < 0$$

where $b = a_1$ in equation (3) and $a = a_0 = 1$, thus we obtain :

$$-\big((\beta_1 + \beta_2)I_a^* + \alpha_1 + \delta_1 + \delta_2 + \gamma_1 + \gamma_2 + 4\mu\big) < 0$$

$$\Leftrightarrow -\frac{(\beta_1 + \beta_2)(\Re_0 - 1)}{\beta_1(\gamma_1 + \gamma_2 + \mu)(\delta_1 + \delta_2 + \mu)(\beta_2 + \mu)} - (\alpha_1 + \delta_1 + \delta_2 + \gamma_1 + \gamma_2 + 4\mu) < 0$$

Let:

$$\mathcal{p} = \beta_1(\gamma_1 + \gamma_2 + \mu)(\delta_1 + \delta_2 + \mu)(\beta_2 + \mu)$$
$$q = (\alpha_1 + \delta_1 + \delta_2 + \gamma_1 + \gamma_2 + 4\mu)$$

We obtain:

$$\Leftrightarrow -\frac{(\beta_1+\beta_2)(\Re_0-1)}{\wp}-q<0$$

$$\Leftrightarrow -(\beta_1+\beta_2)(\Re_0-1)-\wp q<0$$

This condition is satisfied when

$$\Re_0-1>0$$
$$\Re_0>1$$

In a similar manner, it is also obtained that:

$$x_1x_2+x_1x_3+x_1x_4+x_2x_3+x_2x_4+x_3x_4=x=\frac{c}{a}>0$$

where $c=a_2$ in equation (4) and $a=a_0=1$.

$$x_1x_2x_3+x_1x_2x_4+x_1x_3x_4+x_2x_3x_4=-\frac{d}{a}<0$$

where $d=a_3$ in equation (5) and $a=a_0=1$.

$$x_1x_2x_3x_4=\frac{e}{a}>0$$

where $e=a_4$ in equation (6) and $a=a_0=1$.

Based on the analysis, the fourth-degree polynomial satisfies the required conditions, and $\Re_0>1$, which means that the polynomial roots have negative real parts. It has been proven that the endemic equilibrium $\mathcal{E}^*=(S^*,V^*,E^*,I_a{}^*,I_s{}^*,R^*)$ is locally asymptotically stable, indicating that each infected individual has the potential to transmit the infection to several susceptible individuals, leading to an endemic spread of the disease

VI. NUMERICAL SIMULATION

Based on the case study in Jakarta Province with a total population of 10,680,000 individuals [21], numerical simulations will be performed to illustrate the dynamics of COVID-19 transmission. From references [22,23], the following parameter values were obtained:
$\Lambda=416{,}6258;\ \mu=3{,}91389\times10^{-5};\ \beta_1=2{,}00142\times10^{-7};\beta_2=2\times10^{-10};\alpha=0{,}0085;\ \gamma_1=0{,}20441;\ \gamma_2=1{,}07550;\ \delta_1=0{,}32160;\ \delta_2=0{,}6784;\ \sigma_1=1{,}01218;\ \sigma_2=0{,}00001.$

Using the parameter values listed in Table 2 and the given initial conditions, the endemic simulation is presented as follows:
$S(0)=8.138.149, V(0)=10.703.334, E(0)=1.944.154, I_a(0)=1.023.447, I_s(0)=227.433, R(0)=1.234.566.$

The following illustrates the dynamic behavior of the $SVEI_aI_sR$ model (susceptible unvaccinated, susceptible vaccinated, exposed, asymptomatically infected, symptomatically infected, and recovered) in relation to the transmission of COVID-19.

Fig. 2 shows the change in the number of susceptible unvaccinated individuals. At $t=0$, the number of unvaccinated susceptible individuals is approximately 8.140.000. At $t=500$ it decreases to around 48.791. The decline occurs gradually until day 9, while on day 10, a rapid decrease is observed due to the high number of susceptible individuals receiving vaccination and interactions with the asymptomatically infected subpopulation. This leads to susceptible unvaccinated individuals moving into the vaccinated and exposed subpopulations, and over time, the population approaches its equilibrium point around $S_0=48.791$.

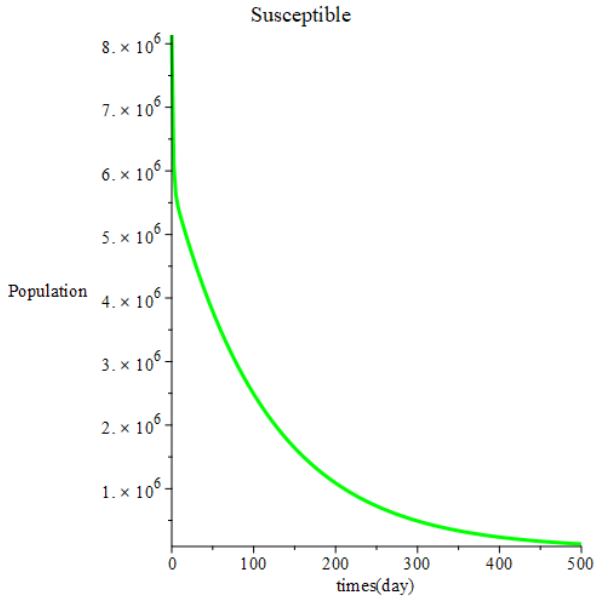

Fig. 2. Plot of The Susceptible Subpopulation Over Time

Fig. 3 shows an increase in the vaccinated subpopulation. Initially (t = 0) the number is approximately 10.700.000 and continues to rise, reaching around 13.800.000 by day 500. This increase occurs due to the large number of susceptible individuals receiving vaccination. Over time, the population gradually approaches its equilibrium point around $V_0 = 13.800.000$.

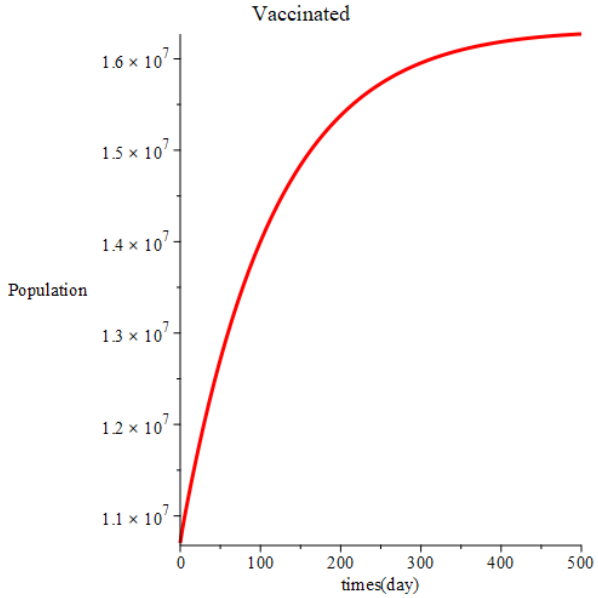

Fig. 3. Plot of The Vaccinated Subpopulation Over Time

Fig. 4 shows the change in the number of exposed individuals. At $t = 0$, the exposed population is approximately 1,950,000, whereas by $t = 20$, it decreases to around 5. This decline occurs because exposed individuals progress to become infected, either asymptomatically or symptomatically. Starting from day 25, the exposed subpopulation begins to stabilize around 0 and gradually decreases toward its equilibrium point at $E_0 = 0$.

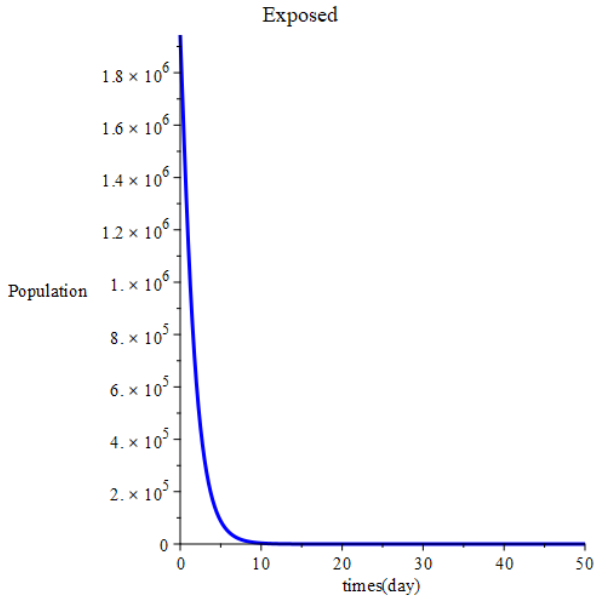

Fig. 4. Plot of The Exposed Subpopulation Over Time

Fig. 5 shows the change in the number of asymptomatically infected individuals. At $t = 0$, this subpopulation is approximately 1,020,000, whereas by $t = 19$, it decreases to around 5. This decline occurs as asymptomatically infected individuals begin to develop symptoms and recover. Starting from day 25, the subpopulation stabilizes around 0 and gradually decreases toward its equilibrium point at $I_{a_0} = 0$.

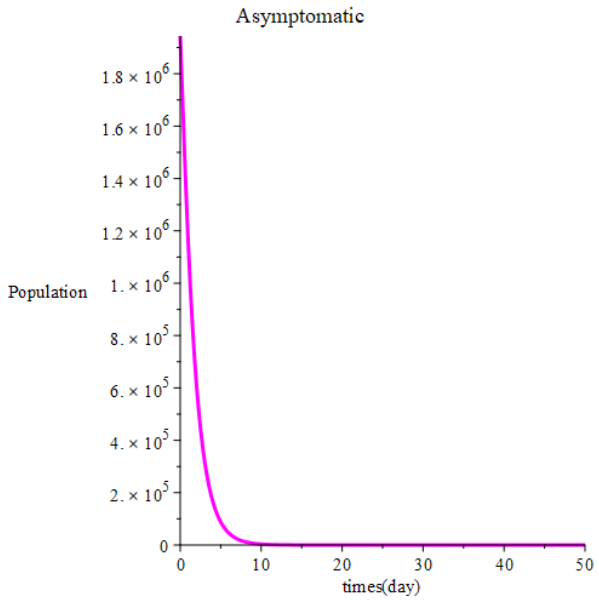

Fig. 5. Plot of The Asymptomatic Subpopulation Over Time

Fig. 6 shows the change in the number of symptomatically infected individuals. At $t = 0$, this subpopulation is approximately 227.500, whereas by $t = 20$, it decreases to around 5. The symptomatically infected subpopulation increases rapidly until day 5, reaching about 1,230,000, and then gradually decreases until day 13. This decline occurs as symptomatically infected individuals recover and some succumb to the infection. Starting from day 26, the

subpopulation begins to stabilize around 0 and gradually decreases toward its equilibrium point at $I_{S_0} = 0$.

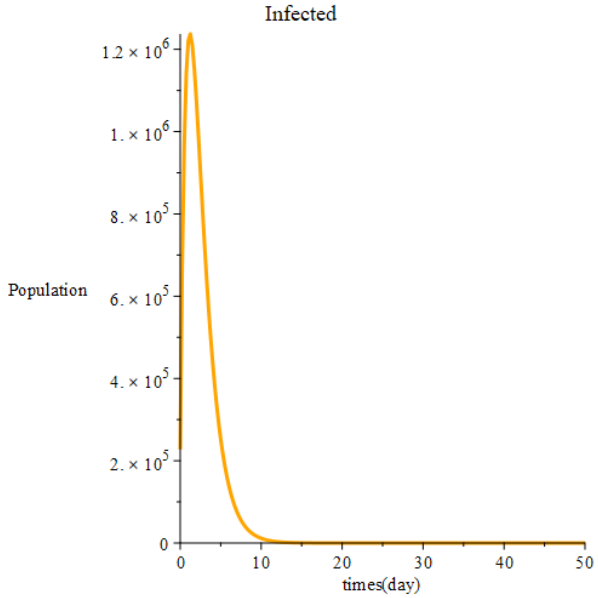

Fig. 6. Plot of The Infected Subpopulation Over Time

Thus, the equilibrium point $\mathcal{E}^0(S_0, V_0, E_0, I_{a_0}, I_{s_0}, R_0)$ is locally asymptotically stable since $\Re_0 < 1$. Consequently, COVID-19 gradually disappears from the population over time.

VII. CONCLUSION

A SVEIR model was developed by incorporating interactions between asymptomatically infected and symptomatically infected individuals. In this study, the spread of COVID-19 depends on the value of $\Re_0$ at the equilibrium point, which helps determine the stability of the model. To analyze the local stability of the disease-free equilibrium, the Routh–Hurwitz method was employed. Based on the analysis, it was found that if $\Re_0 < 1$, the model is locally asymptotically stable at the disease-free equilibrium.

Numerical simulations were also conducted in this study to illustrate the dynamics of COVID-19 transmission. From the simulation results, $\Re_0 = 0.001897843854$, which shows that the COVID-19 transmission model is locally asymptotically stable at the disease-free equilibrium. These results suggest that effective control strategies aimed at reducing the basic reproduction number below unity are essential to eliminate the disease. Therefore, public health stakeholders should focus on interventions that reduce transmission rates, such as minimizing contact between individuals, improving preventive measures, and enhancing early detection and treatment, in order to ensure that the disease eventually disappears from the population.

ACKNOWLEDGEMENTS

This work is supported by the Research Cluster for Mathematical Modeling and Optimization, Diponegoro University, Semarang, Indonesia.

REFERENCES

[1] Yang, C.Y. dan Wang, J. (2020): A mathematical model for the novel coronavirus epidemic in Wuhan, China, *Mathematical Biosciences and Engineering,* 17, 2708-2724.
[2] Widowati, Putro, S. P., Maan, N., Sulpiani, R. (2019): Implementation of lyapunov method to analyze the stability of pompano, cantang growth and nutrition dynamical systems, *Journal of Physics : Conference Series*, 1217, 012059.
[3] Windawati, S., Shodiqin, A., dan Aini, A. N. (2020): Analisis Kestabilan Model Matematika Penyebaran Penyakit Demam Berdarah dengan Pengaruh Fogging. *Square : Journal of Mathematics and Mathematics Education, 2, 1.*
[4] Shen, Z. H., Chu, Y. M., Khan, M. A., Muhammad, S., Al-Hartomy, O. A., Higazy, M. (2021): Mathematical modeling and optimal control of the COVID-19 dynamics, *Results in Physics*, 31, 1-9.
[5] Goswami, N. K., Olaniyi, S., Abimbade, S. F., Chuma, F. M. (2024): A mathematical model for investigating the effect of media awareness programs on the spread of COVID-19 with optimal control, *Heatlhcare Analytics,* 5, 1-15.
[6] Lamwong, J., Wongvanich, N., Tang, I., Pongsumpun, P. (2023): Optimal control strategy of a mathematical model for the fifth wave of COVID-19 outbreak (omicron) in Thailand, *Journal Mathematics,* 2024, 1-29.
[7] Aakash, M., Gunasundari, C., Athithan, S., Sharmila, N. B., Kumar, G. S. (2024): Mathematical modelling of COVID-19 with the effects of quarantine and detection, *Partial Differential Equations in Applied Mathematics,* 9, 1-7.
[8] ElHassan, A., AbuHour, Y., Ahmad, A. (2023): An optimal control model for COVID-19 spread with impacts of vaccination and facemask, *Heliyon,* 9, 1-14.
[9] Paul, A. K., Basak, N., Kuddus, Md. A. (2024): Mathematical analysis and simulation of COVID-19 model with booster dose vaccination strategy in Bangladesh, *Results in Engineering*, 21, 1-26.
[10] Bandekar, S. R. dan Ghosh, M. (2022): Mathematical modelling of COVID-19 in India and its states with optimal control, *Modelling Earth Systems and Environment,* 8, 2019-2034.
[11] Istiqomah, N. A., Widowati, Herdiana, R., Triyana, E. (2022): Stability Analysis of the Covid-19 Spread Model Considering Physical Distancing and Self-Precaution, *International Journal of Advances in Engineering and Management (IJAEM)*, 4, 1, 768-778.
[12] Fitriani, U. A., Widowati, Sutimin, Sasongko, P. S. (2022): Mathematical modeling and analysis of COVID-19 transmission dynamics in Central Java Province, Indonesia, *Journal of Physics: Conference Series* (*ISNPINSA)*, 1943, 012139.
[13] Forrest, U., Al-arydah, M. (2024): Optimal Control Strategies for Infectious Diseases with Consideration of Behavioral Dynamics, *Mathematical Methods in the Applied Sciences,* 48, 1362-1380.
[14] Chen, K., Wei, F., Zhang, X., Jin, H., Wang, Z., Zuo, Y., Fan, K., (2024): Epidemiological Feature Analysis of SVEIR Model with Control Strategy and Variant Evolution, *Infectious Disease Modelling,* 9, 689-700.
[15] Al-arydah, M., (2023): Mathematical Modeling and Optimal Control for COVID-19 with Population Behavior, *Mathematical Methods in the Applied Sciences,* 46, 19184-19198.
[16] Hussain, J., Laldinpuii, J., (2024): Vaccination Strategies Against SARS-CoV-2: Evaluating The Impact Of Coverage and Efficiency Using a Mathematival Model, *Modelling Earth Systems and Environment,*10(5), 5983-6001.

[17] https://corona.jakarta.go.id/ (accessed May. 28, 2022).
[18] Ma, Z. dan Li, J. (2009). *Dynamical Modeling and Analysis of Epidemics*. Singapore: World Scientific Publishing Co. Pte. Ltd.
[19] A. D. Zewdie and S. Gakkhar, "A Mathematical Model for Nipah Virus Infection," J. Appl. Math., vol. 2020, 2020.
[20] Khalil, H. K. (2002). Nonlinear Systems (3rd ed.). Upper Saddle River, NJ: Prentice Hall.
[21] https://jakarta.bps.go.id/ (accessed May. 28, 2022).
[22] Ariyani, R. C. A., Widowati, Kartono, Tjahjana, R. H., Utomo, R. H. S., (2023): Analysis of Local Stability Of The Model On COVID-19 Spread in DKI Jakarta Province, *E3S Web Conf. The* 8^{th} *International Conference on Energy, Environment, Epidemiology and Information System (ICENIS),* 448, 12.
[23] Kumar, R. P., Santra, P. K., Mahapatra, G. S., (2023): Global Stability and Analysing The Sensitivity Of Parameters Of a Multiple-Susceptible Population Model Of SARS-COV-2 Emphasising Vaccination Drive, *Mathematics and Computers in Simulation,* 203, 741-766.